Comparison of Models Having Positive-only Wave CISK with the NICAM Outputs about Eastward Propagation of Super Clusters in the Equatorial Region —Part 2. Approach from a Simplest Model—

YOSHIZAKI Masanori *

キーワード：positive-only wave CISK, super clusters, eastward propagation, equatorial β

Abstract

Using a full model with the positive-only wave CISK to study the eastward-propagating (EP) property of super clusters with a horizontal scale of O (1,000 km) in the tropical areas, Yoshizaki (2016) in Part 1 obtained that the occurrence conditions of splitting disturbances on the top-heavy heating are relaxed when realistic static stability is used. In this study, a mode expansion in the vertical direction is applied to a simplest model in an idealistic troposphere, and linear and nonlinear cases are studied. In the linear case, the propagation property of growing disturbances is separated into two groups: (i) a single slowly westward-propagating one and (ii) splitting ones. However, the (ii)-type disturbances, which lead to the EP property, appear only in the '*unusual*' top-heavy heating compared with observations. It is found that the occurrence conditions for the (ii)-type disturbances become small in the nonlinear case. The nonlinear term mainly causes the upward transport of the potential temperature and helps to enhance the formation of the top-heavy heating. Thus, it is anticipated that the EP property likely appears in the '*usual*' top-heavy heating when complicated models are used in the realistic basic fields, for example, due to the inclusion of the nonlinear term (Part 2) and the adoption of variable static stability (Part 1).

1. Introduction

In the tropics, there are frequently observed organized large-scale precipitation systems (PSs) with specific horizontal and time scales, such as the Madden-Julian Oscillation (MJO; e.g., Madden and Julian 1971; Wheeler and Kiladis 1999) and super clusters (SCs) (e.g., Nakazawa 1988; Takayabu 1994; Wheeler and Kiladis 1999). Among them, SCs have the eastward-propagating (EP) property and an asymmetric east-west structure with a horizontal scale of O (1,000 km) (e.g., Nasuno et al. 2007, 2008). A general detailed introduction is given in Part 1.

To explain the EP property of SCs, many theoretical and numerical studies have been conducted (e.g., Hayashi and Sumi 1986; Takahashi 1987; Lau and Peng 1987; Neelin et al. 1987; Yoshizaki 1991a, 1991b; Yano et al. 1995; Wang and Li 1994; Wang 2005; Mapes 2000; Majda and Shefter 2001; Majda et al. 2004; Khouider and Majda 2006). Although there are advantages and weaknesses as have described in Part 1, a PS view is promoted. Here, the PS view is assumed that the disturbance interacts with the diabatic heating due to precipitation and its physics is inhomogeneous in the horizontal direction. A positive-only wave CISK (POWC) approach (e.g., Hayashi and Sumi 1986; Lau and Peng 1987; Yoshizaki 1991a) can be grouped in the PS view.

A series of the present study aims at how to get splitting disturbances in the '*usual*' top-heavy heating, since Yoshizaki (1991) showed that they are obtained only in the '*unusual*' top-heavy heating as long as an idealistic model is used in the simplified basic field. In Part 1, the EP property of SCs was obtained using a

* Department of Earth-environment Systems, Rissho University

full model with the POWC, and a simplification was made to understand the EP property. It was found that a slowly westward-propagating (WP) disturbance newly emerges from the EP one, when the variable static stability become uniform.

In this study, a simplest model is considered in a simplest basic field, where an idealistic troposphere has a constant speed of sound waves and constant static stability. The investigation of two propagating regimes (a single slowly WP disturbance and splitting ones) is a primary topic. The linear and nonlinear cases are also treated, and the mechanisms enhancing the top-heavy heating by the inclusion of nonlinearity are discussed. To examine the problems noted above, a vertical-mode expansion is applied (Section 2). The propagation property is examined in the linear case in Section 3, and a nonlinear extension is discussed in Section 4. In Section 5, discussion and conclusions are presented.

2. Vertical-mode expansion of the forcing

The governing equations are essentially similar to (1) – (5) in Part 1, although the buoyancy equation (4)' in Appendix is used instead of the θ equation (4) in Part 1. The details are found in Appendix. Here, only different parameters from Part 1 are noted. Q is the forcing defined as $\frac{g\langle\rho\rangle}{\langle\theta\rangle}Q*$. Constant values of <N> and <C_s> are specified as 10^{-2} s^{-1} and 300 ms^{-1}, respectively, but the density variation is included as shown in Fig. 2d of Part 1. The number of vertical grid points is 32, the grid size is uniform as 500 m, and the top height is 16 km.

In this study, a mode expansion of the forcing in the vertical direction is tried, similarly to Yoshizaki (1991a). There are two advantages compared with the grid models in the vertical direction which most researchers used (e.g., Yamasaki 1969, Hayashi 1970, Lau and Peng 1987, Chang and Lim 1988). The first is the linear property in the vertical direction. Compared with Chang and Lim (1988) and so on, the separation between the propagating and non-propagating features can be easily done. The second is a simple treatment of horizontal propagation of each baroclinic modes. A constant speed due to a non-dispersive property is attained for each mode when the hydrostatic assumption is applied on a non-rotating plane.

In a linear case, the variables of mass-weighted winds, mass-weighted buoyancy and pressure can be decomposed into horizontal and vertical parts, and the vertical parts can be separated into two groups: (U', V', p') and (W', B', Q).

The profiles of Q expanded in the vertical direction are shown in Fig. 1. Compared with Q* (solid lines in Fig. 2a in Part 1), the maximum points of Q are located lower because of z dependence of <ρ>. For (W', B', Q), the vertical structure of the n-th baroclinic mode (h_n) can be expressed as

$$\frac{d^2 h_n}{dz^2}+\frac{g}{\langle C_s\rangle^2}\frac{dh_n}{dz}+\left(n^2\pi^2+\frac{g}{4\langle C_s\rangle^2}\right)h_n=0, \qquad (1)$$

where n is a positive integer (n=1, 2, 3,⋯). The analytical solution of (1) is given as

$$h_n(z)=\exp\left(-\frac{g}{2\langle C_s\rangle^2}z\right)\sqrt{2}\sin\left(n\pi\frac{z}{z_T}\right), \qquad (2)$$

where z_T is the top height. This satisfies the following relationship as

$$\frac{1}{z_T}\int_0^{z_T}\exp\left(\frac{g}{\langle C_s\rangle^2}z\right)h_n(z)h_{n'}(z)dz=\delta_{n\,n'}, \qquad (3)$$

where $\delta_{n\,n'}$ is Kronecker's delta (1 for n = n' and 0 for n ≠ n'). These solutions indicate the orthogonal relationship between different n and n'.

This mode expansion in the vertical direction has already been used by Fulton and Schubert (1985), Schubert and Masarik (2006), and Tulich et al. (2007). Compared with previous studies, the present form of (2) is a lower-weighted functional one in the vertical direction. The difference comes from the choice of different variables, i.e., a mass-weighted z-velocity component in the present case $W'(\equiv\langle\rho\rangle w')$ or a z-velocity component in the previous ones, such as w'. Since the amplitude of $\langle\rho\rangle^{\frac{1}{2}}w$ in the isothermal atmosphere is constant in the vertical direction, the amplitude reversal between the present and previous studies can be anticipated.

The mode expansion applied to the vertical profile of Q (Fig. 1a) is approximated as

$$Q(z) = 0.559\, h_1(z) + 0.282\, h_2(z) - 0.053\, h_3(z) - 0.040\, h_4(z) \ldots \qquad (4)$$

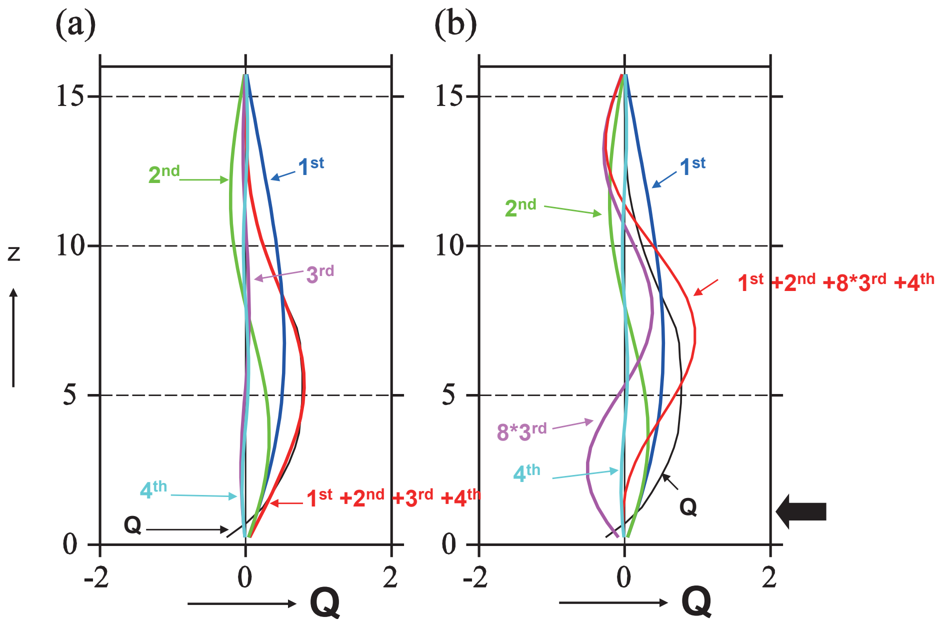

Figure 1 (a) Vertical forcing profiles of (1, 1, 1, 1); first (blue), second (green), third (purple), and fourth (cyan) baroclinic modes, their sum (red), and Q (black) from Q* (solid lines) of Fig. 2a in Part 1. (b) (1, 1, 8, 1). The level of w_B is shown by an arrow.

Except in the lower layer, the sum of these four baroclinic modes can approximately represent the forcing profile. At least, several baroclinic modes are needed to express the realistic vertical profiles of the forcing (diabatic heating). It is noteworthy that the signs of the first and second baroclinic modes are positive at the level of w_B, while those of the third and fourth ones are negative. Hereafter, the dependence of the propagation property is examined on the basis of the combination of the first four baroclinic modes expressed as (1, 1, 1, 1), where each row means $h_n(z)$ from n = 1 in order and the number indicates each amplitude (a_n). For example, (1, 0, 4, 0) means Q = 0.559 h_1 (z) – 0.212 (= 4 x 0.053) h_3 (z). Here, by putting a_1 = 1, a_2 = 1 or 0, and a_4 = 1 or 0, only a_3 (integer) is changed in the interval of 0 to 8. In this study, the baroclinic mode of a_3 is negative at the level of w_B, and its magnitude is considered to determine the whole propagation property. Figure 1b shows an example of a forcing profile with eight times of the 3rd baroclinic mode (1, 1, 8, 1). Although this case is artificially exaggerated ('unusual'), the top-heavy heating profiles, where the heating is intense around the heights of 5 – 10 km, are frequently observed (e.g., Lin et al. 2004).

3. Propagation property in a linear case

As an example of a linear case, Figure 2 shows the longitude - time sections of $\log_{10} |w|$ at z = 3.5 km for (1, 0, 0, 0), (1, 1, 8, 0) and (1, 0. 8, 0). In Fig. 2a, a single nearly stationary growing disturbance is obtained. Hereafter, this is called a slowly WP disturbance because it propagates westward slowly when a longer simulation is made. Such disturbances are seen for a_3 smaller than 7 in (1, 1, a_3, 1), smaller than 8 in (1, 1, a_3, 0), and smaller than 2 in (1, 0, a_3, 0) (dashed lines in Fig. 6). Nearly stationary damped disturbances are also obtained for (0, 1, 0, 0) (not shown). On the other hand, the preferred disturbances in Figs. 2b and 2c are splitting ones. Such splitting disturbances are usually found for cases in which the 3rd baroclinic mode is negatively large at the level of w_B, i.e., a large a_3. Thus, the top-heavy heating profiles are likely to produce splitting disturbances. Consequently, all growing disturbances calculated in this study can be separated into two groups: (i) a single slowly WP disturbance and (ii) splitting ones, as in Takahashi (1987) and Yoshizaki (1991a).

The question of how such a propagation property is determined then needs to be answered. It is shown that the role of each baroclinic mode is determined by the

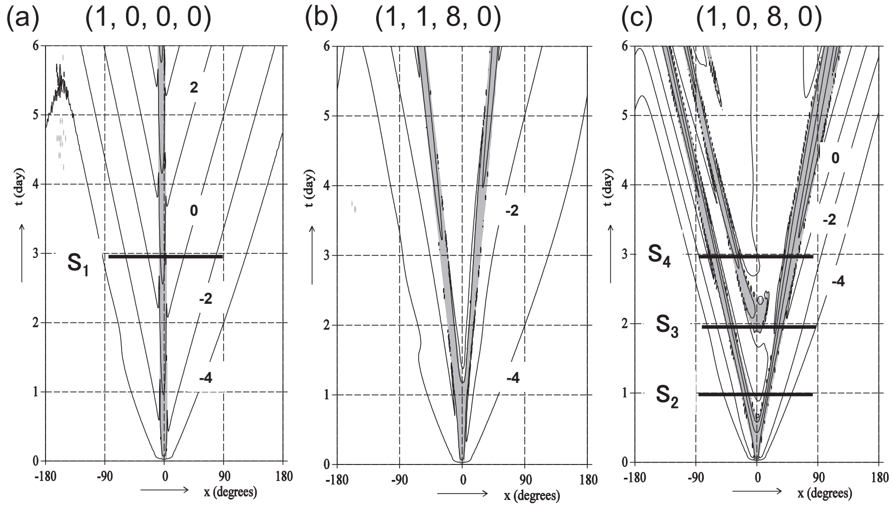

Figure 2 Longitude - time sections of log $_{10}$ | w | at z = 3.5 km in the linear case for (a) (1, 0, 0, 0), (b) (1, 1, 8, 0), and (c) (1, 0, 8, 0) with contour interval of 2. Areas drawn by grey indicate those of upward motion. The horizontal sections along the S_1, S_2, S_3, and S_4 lines are shown in Fig. 3.

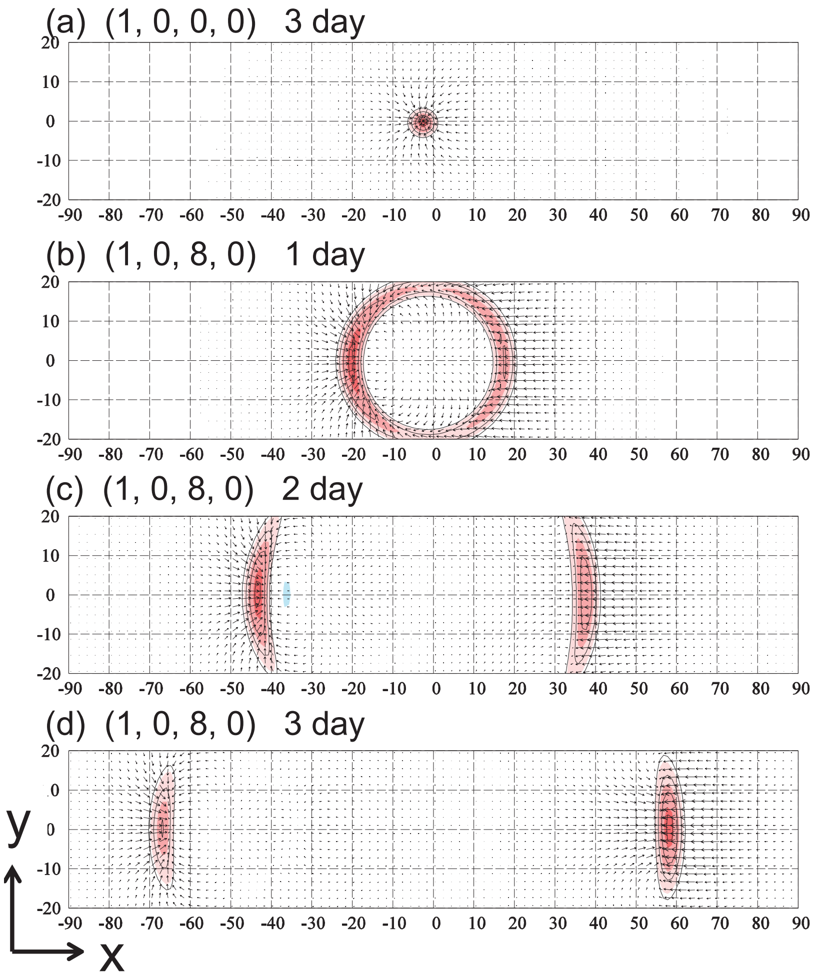

Figure 3 Horizontal structures of vectors (u, v), w (color), and Q (contours) at (a) 3 days for (1, 0, 0, 0), and at (b) 1 day, (c) 2 days, and (d) 3 days for (1, 0, 8, 0). All variables are normalized in each plane.

sign at the level of w_B. Here, we consider (1, 1, 8, 0) in Fig. 2b. When each baroclinic mode is excited independently, the 1st baroclinic mode grows with a slowly WP property (Fig. 2a), while the 2nd baroclinic mode is damped nearly stationary and the 3rd baroclinic mode is also damped (not shown). Although the 2nd and 3rd baroclinic modes are similarly damped, they play different roles. When the 1st and 2nd baroclinic modes are combined as (1, 1, 0, 0…) (not shown), a single slowly WP property appears as (1, 0, 0, 0) (Fig. 2a). When the 1st and 3rd baroclinic modes are combined as (1, 0, 8, 0) (Fig. 2c), on the other hand, splitting disturbances are obtained, as in (1, 1, 8, 0) (Fig. 2b). The difference between the 2nd and 3rd baroclinic modes is the sign at the level of w_B. In (1, 0, 8, 0) (Fig. 2c), the 1st baroclinic mode works for the amplification of the disturbance and the 3rd baroclinic modes work for the propagation. The oscillatory property in the 3rd baroclinic mode, which is originally damped with time due to negative buoyancy at the level of w_B, is excited by the coupling of the 1st baroclinic mode and changes to the propagating one in the horizontal direction.

The results obtained above can be generalized as follows, although they are essentially similar to those in Yoshizaki (1991a). When the signs of baroclinic modes at the level of w_B are all positive or positive and slightly negative, single slowly WP growing disturbances are attained. On the other hand, splitting growing disturbances are obtained when the signs of the baroclinic modes at the level of w_B are both positive and moderately negative. At least, one baroclinic mode should be greater than a threshold magnitude at the level of w_B for preferred disturbances to be unstable. Generally, the top-heavy forcing profile likely induces the propagation property. Therefore, the dynamics of the propagation property reported above are different from those of linear neutral waves controlled by the dispersion relation (e.g., Matsuno 1966).

Figure 3 shows the horizontal patterns of u, v, w, and Q at 1.75 km at 3 days for (1, 0, 0, 0) and at 1, 2 and 3 days for (1, 0, 8, 0). For (1, 0, 0, 0) (Fig. 3a), a quasi-stationary disturbance moving slightly westward has a compact circular shape. For (1, 0, 8, 0) (Figs. 3b, 3c and 3d), on the other hand, a disturbance expands outward in a radial direction first and soon the trapped structure in the latitudinal direction appears due to the equatorial beta. When this behavior is viewed in the longitude - time section, splitting disturbances are attained.

For (1, 0, 8, 0), with time, EP and WP disturbances indicate different behaviors; that is, the EP one is always single, while a new WP one repeatedly occurs on the eastern side of an old disturbance resulting in a wavy train of WP disturbances (Fig. 2c). Such asymmetric horizontal patterns are frequently found in POWC simulations (e.g., Yoshizaki 1991a). This feature was explained by considering a linear response problem for a localized heating propagating in the longitudinal direction by Yoshizaki (1991b). The details are explained in Section 5.

4. Extension to a nonlinear case

a. Nonlinear property

In a nonlinear case, only terms related to ε_1 in Part 1 are added. However, it is assumed that the vertical profile of the Q is unchanged. Figure 4 shows the longitude - time sections of w at z = 3.5 km for (1, 0, 0, 0) and (1, 1, 8, 0). A single slowly WP disturbance is found in Fig. 4a, and splitting disturbances are seen in Fig. 4b. Most cases have propagation properties similar to the linear case, although the obtained amplitudes become complicated and sometimes saturated.

In some cases, however, different propagation properties are found between the linear and nonlinear cases. Figure 5 shows the longitude - time sections of $\log_{10}|w|$ in the linear case and w in the nonlinear case at z = 3.5 km for (1, 1, 5, 1). The linear preferred disturbance grouped into a single slowly WP one (Fig. 5a) differs from the nonlinear preferred ones, in which splitting ones are dominant (Fig. 5b).

The dependence of a_3 on the propagation property in linear and nonlinear cases is summarized in Fig. 6. Here, (1, 0, a_3, 0), (1, 1, a_3, 0), and (1, 1, a_3, 1) are studied. In the linear case, faster propagation is generally obtained in larger a_3 cases of splitting disturbances. However, the occurrence conditions for splitting disturbances are 'unusual'. The term of 'unusual' means that the heating profile is too 'top-heavy' compared with the observations or the NICAM outputs. In the nonlinear cases, on the contrary, the threshold magnitudes from the slowly WP disturbance to splitting ones become smaller than those in the linear case. This suggests that the nonlinear effect not only produces the amplitude saturation of preferred disturbances but also weaken the occurrence condition for slitting disturbances. Because the realistic atmosphere is nonlinear, splitting disturbances are more likely than they are in the linear case.

b. Role of the nonlinear terms to enhance the top-heavy heating

It is necessary to explain why nonlinearity decreases the threshold values. Figure 7 shows the vertical profiles of heat budgets for (1, 1, 5, 1) at 6 days, denoted as ‖ ‖. The areas of intense upward motion are chosen and averaged in the domain of 10° longitude and -4° – 4° latitude. Except for the time change of θ', two terms of $\|Q^*\|$ (heating term) and $\left\|-w'\dfrac{d\bar{\theta}}{dz}\right\|$ (linear term) are dominant in the linear case (Fig. 7a), while three terms of the heating, linear terms, and $\left\|-u'\dfrac{\partial\theta'}{\partial x}-v'\dfrac{\partial\theta'}{\partial y}-w'\dfrac{\partial\theta'}{\partial z}\right\|$ (nonlinear term) dominate in the nonlinear case (Fig. 7b). Since the vertical profiles of the heating and linear terms are similar in both cases, only a nonlinear term is focused on. Compared with these two terms, the nonlinear term has a higher vertical structure; i.e., negative values in the lower troposphere (< 9 km) and positive

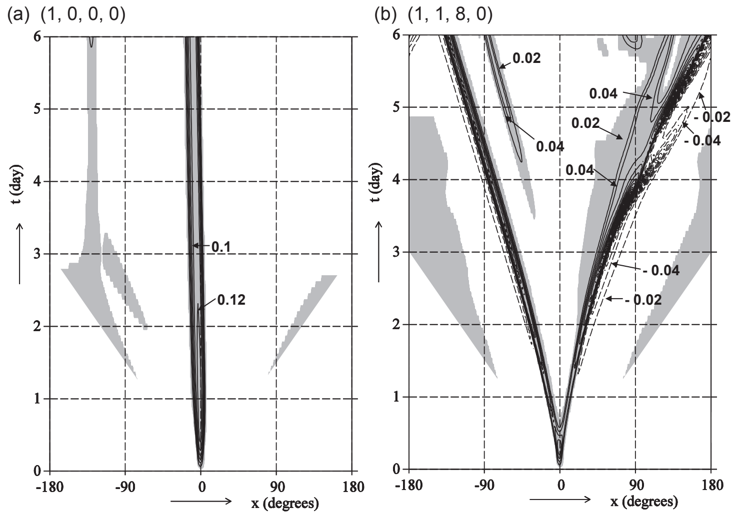

Figure 4 Longitude - time sections of w at z = 3.5 km in the nonlinear case for (a) (1, 0, 0, 0) and (b) (1, 1, 8, 0) with contour interval of 0.02 ms^{-1}. Areas drawn by grey indicate those of upward motion.

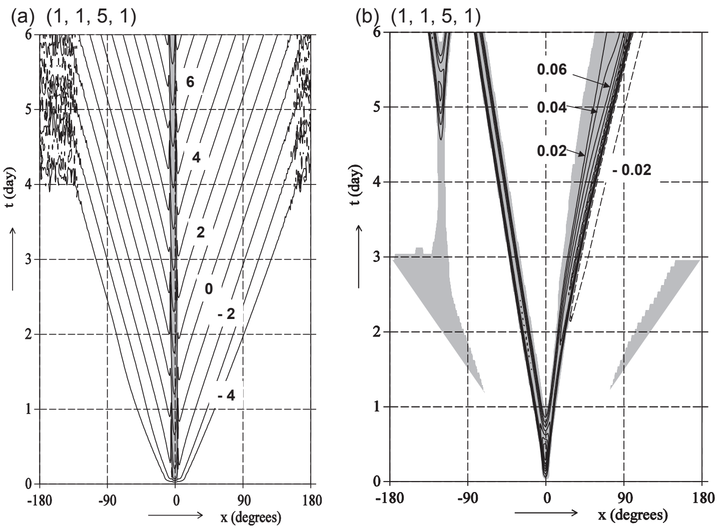

Figure 5 Longitude - time sections of (a) log $_{10}$ | w | with contour interval of 1 in the linear case and (b) w in the nonlinear case at z = 3.5 km with contour interval of 0.02 ms^{-1} for (1, 1, 5, 1). Areas drawn by grey indicate those of upward motion.

values in the upper troposphere. A similar vertical profile is obtained for a quasi-nonlinear case,[1] in which only $\left\| -w'\dfrac{\partial \theta'}{\partial z} \right\|$ is included in the linear case among three terms in the nonlinear term (Fig. 7c). Since the quasi-nonlinear term works to advect θ' upward, the nonlinear case has the tendency of the top-heavy heating more than it does in the linear case. As the top-heavy heating likely induces splitting disturbances, it is concluded that nonlinearity relaxes the occurrence condition for splitting disturbances.

5. Discussion and conclusions

In Part 1, the EP property of SCs in the tropical areas was simulated using a full model with the POWC. However, this is not enough to get a deep understanding of the EP property. Here, a simplest model in an idealistic troposphere with constant static stability and constant speed of sound waves should be discussed from a different standpoint from Part 1.

In this study, the grouping of growing disturbances about propagation was tried. In the linear case, two groups of growing disturbances are obtained as Yoshizaki (1991a) : (i) a single slowly WP one and (ii) splitting ones, depending on the vertical profiles of the heating. When the signs of baroclinic modes at the level of w_B are all positive or positive and slightly negative, a single slowly WP growing disturbance is attained. On the other hand, splitting growing disturbances are obtained when the signs of baroclinic modes at the level of w_B are both positive and moderately negative. At least, one baroclinic mode should be greater than a threshold magnitude at the level of w_B for preferred disturbances to be unstable. The (ii)-type disturbances likely appear in the top-heavy heating, although their

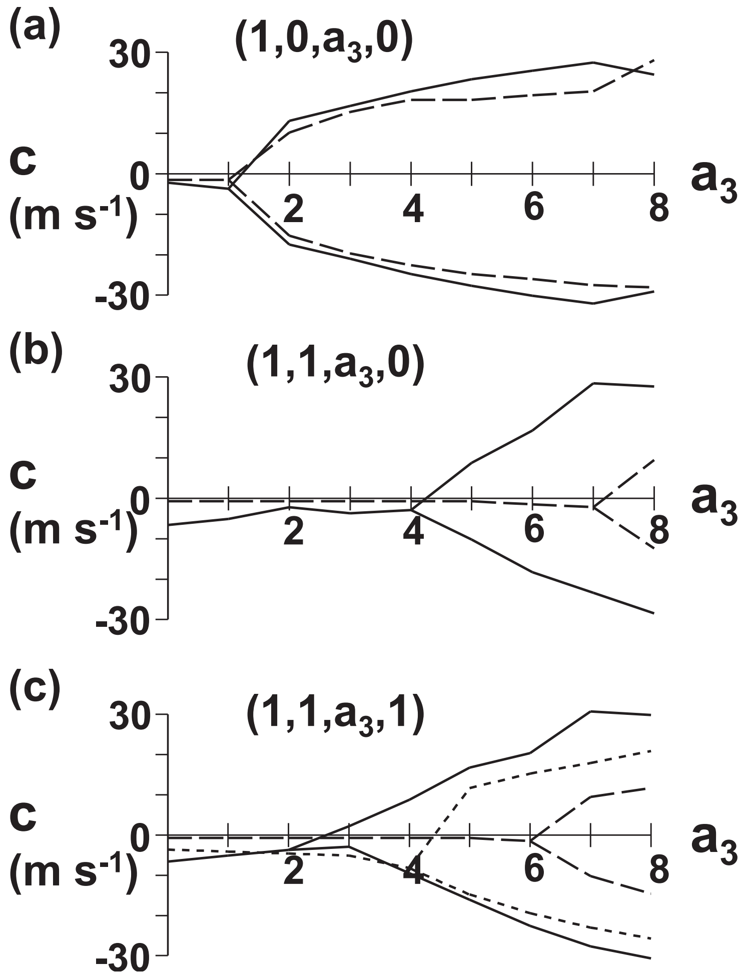

Figure 6 Dependence of the propagation property on the amplitude of the third baroclinic mode (a_3) in the nonlinear (solid) and linear (dashed) cases for (a) (1, 0, a_3, 0), (b) (1, 1, a_3, 0), and (c) (1, 1, a_3, 1). Dotted lines in (c) denote a quasi-nonlinear case.

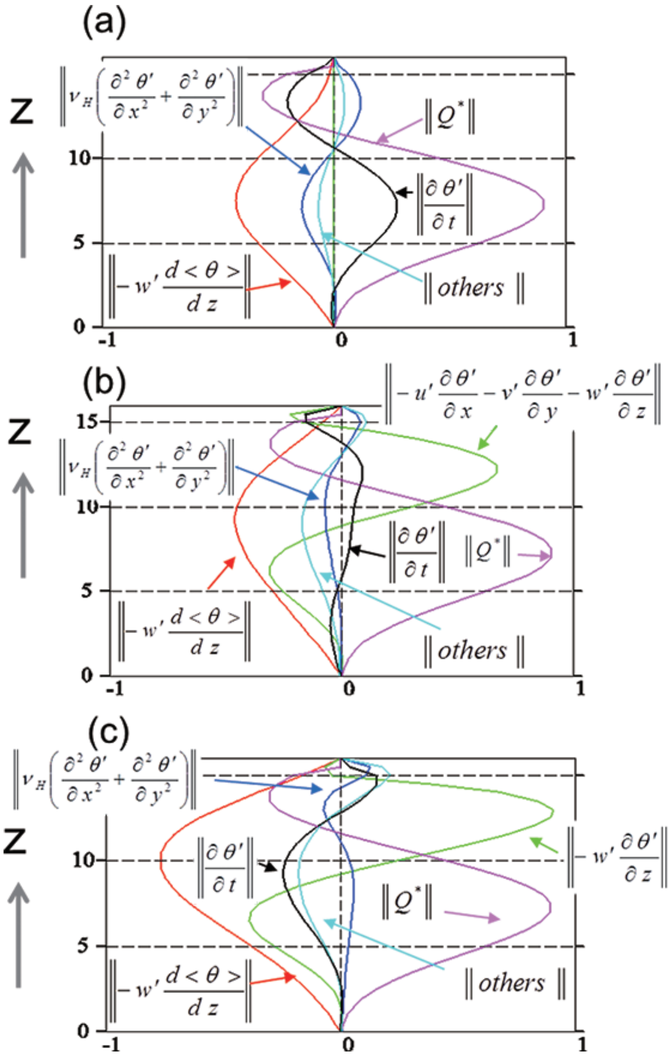

Figure 7 Vertical profiles of heat budgets in (a) linear, (b) nonlinear, and (c) quasi-nonlinear cases for (1, 1, 5, 1) at 6 days, averaged in the domain of 10 degrees in each upward motion; (a) -10° – 0° longitude, (b) 90° – 100° longitude, and (c) 45° – 55° longitude. All variables are normalized in each plane using the maximum values of $||Q^*||$.

occurrence conditions are 'unusual'. In the nonlinear case, meanwhile, these conditions become small. Because the nonlinear term mainly makes the upward transport of the potential temperature, it is concluded that nonlinearity induces the top-heavy heating more than in the linear case.

A series of the present works (Parts 1 and 2) are summarized as follows: A simplest model in an idealistic basic field generally has a (i)-type WP disturbance in a 'usual' top-heavy heating (Part 2). On the other hand, a full model in realistic basic fields (with the 'usual' top-heavy heating) simulates the EP disturbances, which originate from (ii)-type splitting ones (Part 1). From these results, it is anticipated that the vertical profiles of the top-heavy heating are enhanced as the model becomes complicated and the basic fields used become realistic. That is, the inclusion of the nonlinear term (Part 2) and the adoption of variable static stability (Part 1) help to induce the top-heavy heating and the (ii)-type splitting disturbances are likely realized in the 'usual' top-heavy heating.

Then, why is only EP property chosen from (ii)-type splitting disturbances? One candidate explanation for this question is an asymmetric selection between the EP and WP disturbances in the top-heavy heating due to the equatorial beta (Yoshizaki 1991a, 1991b). In the linear theories (Yoshizaki 1991b), the growing EP and WP disturbances in the POWC cases correspond to a response problem of the EP and WP localized heating in the Rayleigh damping / Newtonian cooling. When the horizontal distributions of the heating are approximated from the POWC outputs, it is found in the response problem that the EP prescribed heating enhances an upward motion only on the heating area, while the WP prescribed heating generates upward motions on the heating area as well as on its eastern side. In the POWC instability case, the EP and WP disturbances have different destinies after the response patterns become large. The EP disturbance grows without hindrance keeping in an isolated manner, while the WP disturbance makes a wavy train of disturbances on its eastern side, reducing its growth more significantly than the EP one. Due to this east-west asymmetric feature (for example, Fig. 2c), the EP disturbance is selected as a preferred disturbance.

Finally, the necessary conditions for the realization of the EP property as like observed SCs are summarized; 1) full models with the driving heating such as the POWC, 2) the realistic basic fields, 3) the equatorial beta, and 4) large-scale disturbances. In this manner, the EP property of PSs observed in the tropics can be simply understood as a response of the localized heating moving in the longitudinal direction.

Appendix:

Using the same definitions and assuming $\varepsilon_1 = \varepsilon_2 = 0$ from (1)-(5) in Part 1, the governing equations are written as

$$\frac{\partial U'}{\partial t} = -\frac{\partial p'}{\partial x} + \beta y V' + \nu_H \Delta_H U' - rU', \qquad (1)'$$

$$\frac{\partial V'}{\partial t} = -\frac{\partial p'}{\partial y} - \beta y U' + \nu_H \Delta_H V' - rV', \qquad (2)'$$

$$0 = -\frac{\partial p'}{\partial z} - \frac{g}{\langle C_s \rangle^2} p' + B', \qquad (3)'$$

$$\frac{\partial B'}{\partial t} = -W' \langle N \rangle^2 + Q + \nu_H \Delta_H B' - rB', \quad and \qquad (4)'$$

$$\frac{\partial U'}{\partial x} + \frac{\partial V'}{\partial y} + \frac{\partial W'}{\partial z} = 0. \qquad (5)'$$

Only the buoyancy equation (4)' is used, instead of the θ equation. Here, $\langle N \rangle^2$ and $\langle C_s \rangle^2$ are constants, and Q is newly defined as $\frac{g\langle\rho\rangle}{\langle\theta\rangle}Q^*$. By putting

$$\begin{pmatrix} U' \\ V' \\ p' \end{pmatrix} = \begin{pmatrix} \tilde{u}(t,x,y) \\ \tilde{v}(t,x,y) \\ \tilde{\phi}(t,x,y) \end{pmatrix} f(z), \quad \begin{pmatrix} W' \\ B' \\ Q \end{pmatrix} = \begin{pmatrix} \tilde{w}(t,x,y) \\ \tilde{b}(t,x,y) \\ \tilde{q}(t,x,y) \end{pmatrix} h(z)$$

and considering the combination of (3)' and (5)', a following equation about the vertical part is derived:

$$\frac{d^2 h}{d z^2} + \frac{g}{\langle C_s \rangle^2} \frac{d h}{d z} + c h = 0, \qquad (6)'$$

where c is a constant. Here, f (z) is proportional to $\frac{dh}{dz}$. The solution of (6)' is given to satisfy the boundary conditions; h (0) = h (z_T) = 0, where 0 and z_T are the positions at the lower and upper boundaries, respectively:

$$h_n(z) = \exp\left(-\frac{g}{2\langle C_s \rangle^2} z\right) \sqrt{2} \sin\left(n\pi \frac{z}{z_T}\right), \qquad (7)'$$

where n is a positive integer. Using (7)', (6)' can be rearranged as

$$\frac{d^2 h_n}{d z^2} + \frac{g}{\langle C_s \rangle^2} \frac{d h_n}{d z} + \left(n^2 \pi^2 + \frac{g}{4\langle C_s \rangle^2}\right) h_n = 0. \qquad (8)'$$

References

Chang, C.-P., and H. Lim, 1988: Kelvin wave-CISK: A possible mechanism for the 30-50 day oscillations. *J. Atmos. Sci.*, **45**, 1709-1720.

Fulton, S. R. and W. H. Schubert, 1985: Vertical normal transformations: Theory and application. *Mon. Wea. Rev.*, **113**, 647-658.

Gill, A. E., 1980: Some simple solutions for heat-induced tropical circulation. *Quart. J. Roy. Meteor. Soc.*, **106**, 447-462.

Gill, A. E., 1982: *Atmosphere-Ocean Dynamics*. Academic Press, 662pp.

Hayashi, Y., 1970: A theory of large-scale equatorial waves generated by condensation heat and accelerating the zonal wind. *J. Meteor. Soc. Japan*, **48**, 140-160.

Hayashi, Y, -Y. and A. Sumi, 1986: The 30-40 day oscillations simulated in an "aqua-planet" model. *J. Meteor. Soc. Japan*, **64**, 451-467.

Lau, K. –M. and L. Peng, 1987: Origin of low-frequency (intraseasonal) oscillations in the tropical atmosphere. Part I: Basic theory. *J. Atmos. Sci.*, **44**, 950-972.

Khouider, B. and A. J. Majda, 2006: A simple multicloud parameterization for convectively coupled tropical waves. Part 1: Linear analysis. *J. Atmos. Sci.*, **63**, 1308-1323.

Madden, R. and P. Julian, 1971: Detection of a 40-50 day oscillation in the zonal wind in the tropical Pacific. *J. Atmos. Sci.*, **28**, 702-708.

Majda, A. J. and M. G. Shefter, 2001: Waves and instabilities for model tropical convective parameterizations. *J. Atmos. Sci.*, **58**, 896-914.

Majda, A. J., B. Khouider, G. N. Kiladis, K. H. Straub and M. G. Shefter, 2004: A model for convectively coupled tropical waves: Nonlinearity, rotation, an comparison with observations. *J. Atmos. Sci.*, **61**, 2188-2205.

Mapes, B. E., 2000: Convective inhibition, subgrid-scale triggering energy, and stratiform instability in a toy tropical wave model. *J. Atmos. Sci.*, **57**, 1515-1535.

Matsuno, T., 1966: Quasi-geostrophic motions in the equatorial area. *J. Meteor. Soc. Japan*, **44**, 25-43.

Nakazawa, T., 1988: Tropical super clusters within intraseasonal variations over the western Pacific. *J. Meteor. Soc. Japan*, **66**, 823-839.

Nasuno, T., H. Tomita, S. Iga, H. Miura and M. Satoh, 2007: Multiscale organization of convection simulated with explicit cloud processes on an aquaplanet. *J. Atmos. Sci.*, **64**, 1902-1921.

Nasuno, T., H. Tomita, S. Iga, H. Miura and M. Satoh, 2008: Convectively coupled equatorial waves simulated on an aquaplanet in a global nonhydrostatic experiment. *J. Atmos. Sci.*, **65**, 1246-1265.

Neelin, J. D., I. M. Held and K. H. Cook, 1987: Evaporation-wind feedback and low-frequency variability in the tropical atmosphere. *J. Atmos. Sci.*, **44**, 2341-2348.

Schubert, W. H. and M. T. Masarik, 2006: Potential vorticity aspects of the MJO. *Dyn. Atmos. Oceans,* **42**, 127-151.

Takahashi, M., 1987: A theory of the slow phase speed of the intraseasonal oscillation using the wave-CISK. *J. Meteor. Soc. Japan,* **65**, 43-49.

Takayabu, N. Y., 1994: Large-scale cloud disturbances associated with equatorial waves. Part I: Spectral features of the cloud disturbances. *J. Meteor. Soc. Japan*, **72**, 433-449.

Tulich, S. N., D. A. Randall and B. E. Mapes, 2007: Vertical-mode and cloud decomposition of large-scale convectively coupled gravity waves in a two-dimensional cloud-resolving model. *J. Atmos. Sci.*, **64**, 1210-1229.

Wang, B. and T. Li, 1994: Convective interaction with boundary-layer dyanamics in the development of a tropical intraseasonal system. *J. Atmos. Sci.*, **51**, 1386-1400.

Wang, B., 2005: Theory, In *Intraseasonal Variability in the Atmosphere-Ocean Climate System*, edited by W. K. M. Lau and D. E. Waliser, Praxis, Chichester, U.K., 307-360.

Yamasaki. M., 1969: Large-scale disturbances in a conditionally unstable atmosphere in low latitude. *Pap. Meteor. Geophys.*, **20**, 289-336.

Yano, J. -I, J. C. McWilliams. M. W. Moncrieff and K. A. Emanuel, 1995: Hierarchical tropical cloud systems in an analog shallow-water model. *J. Atmos. Sci.*, **52**, 1723-1742.

Yoshizaki, M., 1991a: Selective amplification of the eastward-propagating mode in a positive-only wave-CISK model on an equatorial beta plane. *J. Meteor. Soc. Japan*, **69**, 353-373.

Yoshizaki, M., 1991b: On the selection of eastward-propagating modes appearing in the wave-CISK model as tropical intraseasonal (30-60-day) oscillations.-Linear response to localized heating moving in the east-west direction on an equatorial beta plane. *J. Meteor. Soc. Japan*, **69**, 595-608.

Yoshizaki, M., 2016: Comparison of models having positive-only wave CISK with the NICAM outputs about eastward propagation of super clusters in the equatorial region: Part 1. Approach from a full model. *Bulletin of Geo-Environmental Sci.*, **18**, 1-14.

Footnotes:

1) Generally speaking, stable calculations and similar patterns to those of the nonlinear case are obtained only for the quasi-nonlinear case with the upward advection of θ'. The cases with other nonlinear terms sometimes lead to computational instability or show complicated patterns.

赤道域のスーパークラスタの東進に関するNICAMの計算結果とpositive-only wave CISKを持つモデルの比較．Part 2. 単純モデルからのアプローチ

吉　﨑　正　憲[*]

[*]立正大学・地球環境科学部

要　旨：

第1部（Yoshizaki、2016）では、positive-only wave CISK を持つフルモデルを用いて、熱帯域の水平スケール約1000kmのスーパークラスタの東進特性を調べ、大気安定度の鉛直分布を実況に近くすると、もっともらしいtop-heavyな熱源分布で、じょう乱は東西に分かれ東進じょう乱が選択された。ここでは、理想化された対流圏の場でもっとも単純なモデルに鉛直方向のモード展開を適用し、線型および非線型の場合についてtop-heavyな熱源分布とじょう乱の伝搬特性を調べた。線型の場合、成長する擾乱の伝搬特性は、（i）一つの擾乱がゆっくりと西進するタイプと（ii）東西に二つに分かれて伝搬するタイプの二つに分かれた。しかしながら、東進する擾乱に相当する（ii）のタイプは、第1部でみたように‘非常に大きい’top-heavyな熱源分布のときだけあらわれた。それに対して、非線型にすると、（ii）のタイプの発生条件が緩くなった。非線型にすると、擾乱による温位の上層への輸送が起こり、top-heavyな熱源分布になるためである。実況に近い大気安定度や非線型の導入によりtop-heavyな熱源分布の条件が緩和したことから、複雑なモデルと実況に近い環境場を用いれば、東進特性は通常のtop-heavyな熱源分布でも発現すると期待される。

キーワード：positive-only wave CISK、スーパークラスター、東進特性、赤道ベータ